Research Journal of Applied Sciences 1 (1-4): 33-37, 2006

Methods Engineering Thermal for Non Destructive Detection of the Defects in Materials and Structures

[1,2]Ahmed Tafraoui and [1]Soltane Lebaili
[1]Laboratory of Sciences and Engineering of Materials (LSGM),
University of Sciences and Technology, Haouari Boumediene
BP.32 El-Alia, Bab-Ezzouar Algiers (16111), Algeria
[2]Department of Engineering Mechanical, University Centre of
Bechar, BP.417 Bechar (08000), Algeria

Abstract: Several Non-Destructive techniques were applied in the quality control as radiography (x-rays), acoustic signals, and the radioactivity (gamma rays), among these techniques, that of infra-red thermography. Nevertheless in several situations as the industrial quality control, it is very important to use the technique of infra-red thermography in order to examine quantitative information starting from the images of infra-red. The numerical and experimental examination of a circular sample with porosities intern in materials and structure gave results on various positions and dimensions of porosities. The samples used as example are steel, aluminium, ceramics and the pellets of Uraninite (UO_2).

Key words: Method ADI, defect, porosity, method of thermography infra-red

INTRODUCTION

The quality control with Non-Destructive techniques is increasingly more important for much application industrial (aviation, electronics, materials, nuclear industry, civil engineering….etc). A particular Non-Destructive technique consists in subjecting the structure which one wants to examine with a thermal process and to measure the surface distribution of temperature, for example technique of infra-red thermography. The possible surface deformations of the temperature can reveal the presence of internal porosities. In order to increase the possibilities of detection and to be able to obtain quantitative information on the internal defects, it is necessary to be prepared of mathematical models of simulation suitable and precision of the thermal process in the system. To have more information on porosity, we determine its various positions and dimensions inside the sample.

In this present study, we will take as model a circular thick plate with internal porosities for materials and metals, tandisque in nuclear industry; we work on Uraninite pellets (UO_2) to the presence of internal porosities formed during sintering[1-3].

MATERIALS AND METHODS

Mathematical definition of the studied problem: The presence of porosity is revealed by the determination of the surface distribution of the temperature by solving the thermal equation of conduction with the boundary conditions in no stationary mode. Porosity is detected by its position, its thickness. The physical model taken as example is a circular sample[4,5].

Mathematical model: The mathematical equation of the model is the differential equation of thermal conduction without internal source in the no stationary mode:[6].

$$\frac{\partial^2 T}{\partial x^2} + \frac{\partial^2 T}{\partial y^2} = \frac{1}{a}\frac{\partial T}{\partial t} \quad (1)$$

of which:

$$\alpha = \frac{\lambda}{\rho c_p}$$

Corresponding Author: Soltane Lebaili, Laboratory of Sciences and Engineering of Materials (LSGM) University of sciences and Technology Haouari Boumediene BP.32 El-Alia, Bab-ezzouar Algiers (16111), Algeria

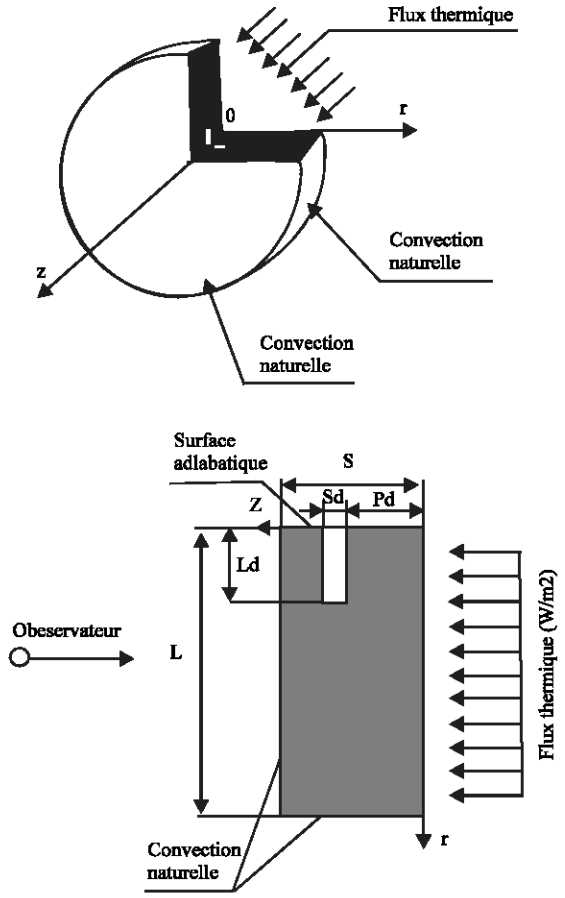

Fig. 1: Representation of artificial porosity

α : Thermal Diffusivity [m^2/S].
λ : Thermal conductivity [W/m°k].
C_P : Specific heat [J/kg°k].
ρ : Density [kg/m^3].
T = T (x, y, t) : temperature of the body.

The two-dimensional model in no stationary mode represented in the co-ordinates cylindrical is:

$$\frac{\partial^2 T(r,z,t)}{\partial r^2} + \frac{\partial^2 T(r,z,t)}{\partial z^2} = \frac{1}{\alpha}\frac{\partial T(r,z,t)}{\partial t} \qquad (2)$$

The circular sample is subjected to a constant flow α on side, on other surfaces a natural convection (h) is imposed. Because of symmetry compared to axis Z where R = 0 to see Fig. 1, we study half of the plate. The geometry of the problem as well as the boundary conditions is represented on the figure Fig. 1.

The boundary conditions on the borders are:

$$\begin{cases} z=0: \; q=-\lambda\dfrac{\partial T}{\partial Z} & (1a) \\ z=s: \; h(T-T\infty)=-\lambda\dfrac{\partial T}{\partial Z} & (1a) \\ r=0: \; \dfrac{\partial T}{\partial r}=0 & (1a) \\ r=L: \; h'(T-T\infty)=-\lambda\dfrac{\partial T}{\partial r} & (1a) \end{cases}$$

To make the result more general, one replaces all the sizes by adimensional sizes:[7].

$$t^* = Fo = \frac{\alpha \times t}{S^2}$$

$$\theta = \frac{T - T\infty}{\frac{q \times s}{\lambda}}$$

$$r^* = \frac{r}{s}$$

$$Sd^* = \frac{Sd}{s} \times 100$$

The Eq. 2 in the adimensional form becomes then:

$$\frac{\partial^2 \theta}{\partial r^{*2}} + \frac{\partial^2 \theta}{\partial z^{*2}} = \frac{\partial \theta}{\partial t^*} \qquad (3)$$

Also, the boundary conditions (1.a-d) are written in the form: With Bi = h×s/λ and Bil = h'×s/λ numbers of biot

$$Z^* = 0 : \frac{\partial \theta}{\partial Z^*} = -1 \qquad (2.a)$$

$$Z^* = 1 : -Bil \times \theta = \frac{\partial \theta}{\partial Z^*} \qquad (2.b)$$

$$r^* = 0 : \frac{\partial \theta}{\partial r^*} = 0 \qquad (2.c)$$

$$r^* = \frac{L}{S} : -Bil \times \theta = \frac{\partial \theta}{\partial r^*} \qquad (2.d)$$

Then the mathematical model is represented by the Eq. 3 with the equations of the boundary conditions (2.a-d)[8,9].

Numerical methods utilisees for the resolution of the mathematical model: We used two methods of numerical resolution:

- The method clarifies simple[10].
- Method ADI (alternating direction implicit method)[11,12].

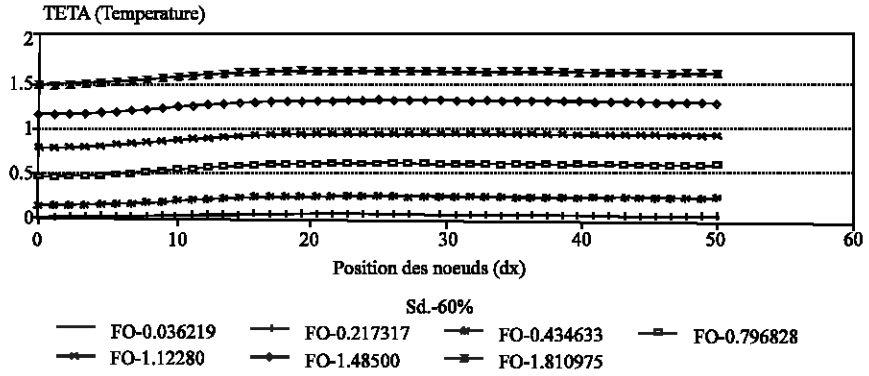

Fig. 2: Results of the ADI method (stainless steel). Distribution of the temperature en function of X

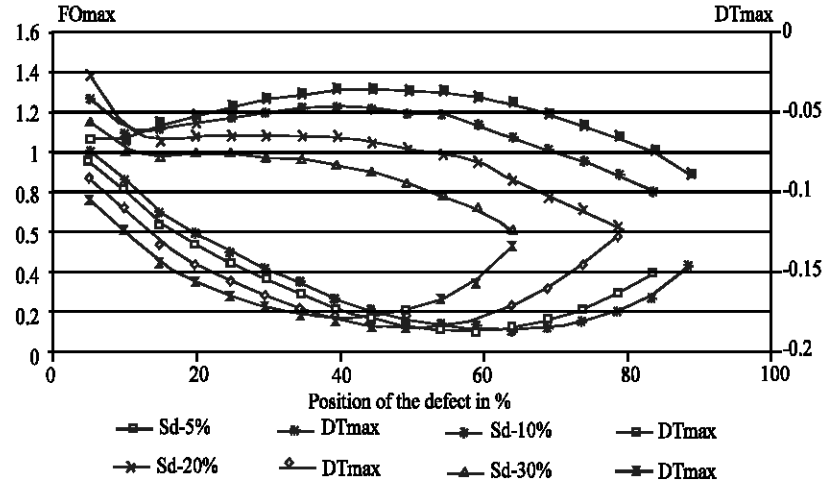

Fig. 3: Result of the ADI method (Aluminum)

Note: It is necessary to pay attention to the calculation of the time limits. The time limits are smallest time given by the stability conditions. $\Delta t^{*} \leq \Delta t^{*}_{limit}$.

The resolution by method ADI leads us to the resolution of a system tridiagonal. This system is solved by the algorithm of Thomas[13].

The data-processing program: Two programs were established for the resolution of the problem in question, one program for the resolution by the explicit method and that of method ADI[14].

RESULTS AND DISCUSSIONS

After having posed and having defined the mathematical model and after the establishment of the simulation program describing the problem, we collect the results of some examples of application (steel, aluminium, ceramics, Uraninite (UO_2)). Let us introduce the characteristics geometrical and physical material and porosity (S, L, Sd, Pd) .A each fixed Sd thickness and with positions different Pd from porosity, we have the results of the surface distribution of the ΔTmax temperature and the values of the number of corresponding Fomax Fourier. With each position Pd of porosity, us will take values maximum of Fo and ΔT for different moments i.e. that we stop the execution of the program when the difference in surface temperature ΔT is maximum (test of convergence), Fig. 2.

What enables us to trace a graph of Fomax and ΔTmax according to the various positions Pd with each Sd thickness in order to be able to determine the optimal time of detection between thermal diffusivities of material and porosity, the position and the characteristics of porosity. The calculation programme based on the model and the digital technique previously described was launched on a microcomputer. The parameters of the data are dimensions of the sample and porosity, their intervals of discretization second, their axes Z and R, the thermophysical characteristics of material of the

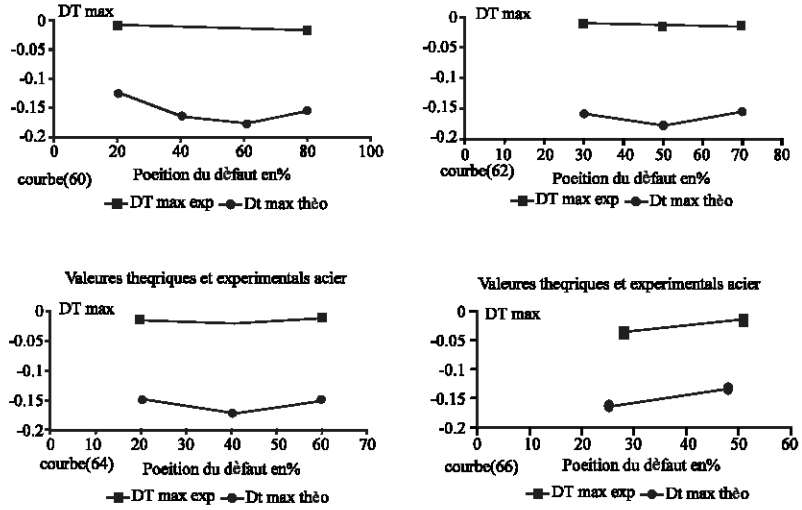

Fig. 4: Results of the ADI method. stainless steel

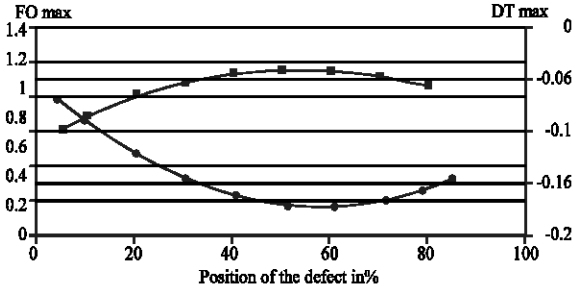

Fig. 5: Results of the ADI method ceramic alumina (AL_2O_3)

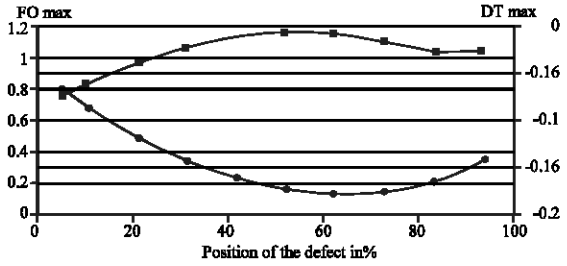

Fig. 6: Values theoretical and experimental. stainless steel

sample and porosity, the convection coefficient and the step of time.

The adimensional numerical results, in particular the couple (Fomax, ΔTmax), for many combinations the thicknesses Sd* and depths Pd* of porosity, were represented in graphs. See Fig. 3, 5, and 6 of the treated examples.

We note a difference from 10% to 15% between the theoretical studies and that experimental presented on the Fig. 4.

Example 1: (Stainless steel 18,6% Cr; 9,5% Ni; 1,11%Mn; 0,46% Si; 0,063% C; 0,023% P).

Example 2: Iron[15].

CONCLUSION

The goal of this work is to estimate the presence of porosities inside metallic material or different by means of research thermography of transition. The analysis was led for various thicknesses of porosities and various positions, in parallel we carried out a digital model with the finished differences representative of heat exchange conductive inside the sample.

In the digital model, we suppose to impose on the one of the two plane faces of the sample a constant heat flux, and we carry out the taking away of the temperatures. We thus create on such surface a heat gradient between the centre and the edge. The digital model confirms the validity of such obvious assertion. Moreover, the couple of the values of thermal moment of visibility maximum are single, i.e., there are never two identical couples representing of dimensions various and localizations different from porosity.

LIST LEGENDS

Symbols	Designations	units
λ*	Thermal conductivity	[_w / m K]
CP	Specific heat	[_J / kg K]

ρ	Density	[_kg / m^3]
α	Diffusivity has	[_m^2 / S]
T (x, y, t)	Temperature of the solid.	[°K]
∂	Differential operator.	
r	Axis of symmetry.	[m]
Z	Axis of symmetry.	[m]
S	Thickness of the plate.	[m]
L	Length of the plate.	[m]
Sd	Thickness of the defect.	[m]
Pd	Depth of the defect.	[m]
Ld	Length of the defect.	[m]
t^* fo	Number of Fourier (adimensional time	
θ (R, Z, T)	Adimensional Temperature.	
r^*	Coordinated adimensional.	
Z^*	Coordinated adimensional.	
Sd^*	Adimensional Thickness of the defect in %.	
Pd^*	Adimensional Depth of the defect in %	
T∞	Temperature of the fluid.	[°K]
h,h ′	Convection coefficients	[_ w/m^2 K]
Bi, Bil	Numbers of Biot.	
q	Quantity of the flux	[_w/m^2]
ΔT^*	Variation of adimensional time.	
Δθ	Variation in the adimensional temperature.	
φ	Heat flux	[W].

REFERENCES

1. Vavilov, V., 1992. Thermal non destructive testing: Short history and state-of-art, A thermografic method eurotherm seminar 27, QIRT, pp: 7-9.
2. Varis, J., J. Hartikaien, R. Lehtiniemi and M. Luukkala, 1992. A simple transportable imaging system for fast thermal Non-Destructive testing, A thermografic method eurotherm seminar 27, QIRT pp: 7-9.
3. Vavilov, V., P.G. Bison, C. Bressan, E. Grinzato and S. Marinetti, 1992. Some new ideas in dynamic thermal tomography, QIRT.
4. Karapez, J.C., D. Bosher, P.H. Delpech, A. Deom, G. Gardette and D. Balageas, 1992. Time-resolved pulsed stimulated infrared thermography applied to carbon-epoxy non destructive evaluation, A thermografic method eurotherm seminar 27, QIRT, pp: 7-9.
5. Vavilov, V., 1992. Transient thermal NDT, conception in formulae, A thermografic method eurotherm seminar 27, QIRT, pp: 7-9.
6. Carslaw, H.S. and J.C. Jaeger, 1982. Conduction of Heat in Solids, Tome 2 la conduction (suite et appendices), Éditeur Gaetan morin.
7. Leontiev, A., Théorie des échanges de chaleur et masse, Editions Mir moscou.
8. Thibault, V., 1984. A three-dimensional numerical method Based on the superposition principal, Numerical Heat Transfer, pp: 127.
9. Fogiel, M., 1988. The heat Transfer problem Silver, published by Macmillan Education LTD, USA .
10. Godounov, S. and et V. Riabenki, Schémas aux différences (OPU).
11. Taine, J. and et J. Peti, 1989. Transferts Thermiques, Mécanique des fluides anisothermes, Dunod université Paris.
12. Nogotov, E.F., Appliquatios of Numerical Heat Transfer, McGraw-Hill.
13. Thibault, J., 1985. Comparaison of nine three-dimensional numerical methods for the solution of the heat diffusion, Equation-num-heat transfer.
14. Anderson, D.A. and et J.C. Tannehill, 1984. Computational Fluid Mechanics and Heat transfer.
15. Ashby, M.F. and et D.R.H. Jones, 1991. Matériaux 2, Microstructure et mise en œuvre, Edition dunod.